© 1996 Oxford University Press
Nucleic Acids Research, 1996, Vol. 24, No. 4 713–720

Atomic force microscopy of long and short double-stranded, single-stranded and triple-stranded nucleic acids

Helen G. Hansma*, Irene Revenko, Kerry Kim and Daniel E. Laney

Department of Physics, University of California, Santa Barbara, CA 93106, USA

Received October 5, 1995; Revised and Accepted December 21, 1995

ABSTRACT

Atomic force microscopy (AFM, also called scanning force microscopy) is proving to be a useful technique for imaging DNA. Thus it is important to push the limits of AFM imaging in order to explore both what types of DNA can be reliably imaged and identified and also what substrates and methods of sample preparation are suitable. The following advances in AFM of DNA are presented here. (i) DNA molecules as short as 25 bases can be seen by AFM. The short single-stranded DNAs imaged here (25 and 50 bases long) appeared globular in the AFM, perhaps because they are all capable of intramolecular base pairing and because the DNAs were in a Mg(II) buffer, which facilitates intramolecular cross-bridging. (ii) AFM images in air of short double-stranded DNA molecules, 100–200 bp, gave lengths consistent with A-DNA. (iii) AFM images of poly(A) show both short bent lumpy molecules with an apparent persistence length of 40 nm and long straight molecules with an apparent persistence length of 600 nm. For comparison, the apparent persistence length for double-stranded DNA from ϕX-174 under the same conditions was 80 nm. (iv) Structures believed to be triple-stranded DNA were seen in samples of poly(dA)·poly(dT) and poly(dG)·poly(dC). These structures were twice as high as double-stranded DNA and the same width. (v) Entire molecules of lambda DNA, ~16 μm long, were imaged clearly in overlapping scans. (vi) Plasmid DNA was imaged on oxidized silicon, although less clearly than on mica.

INTRODUCTION

Atomic force microscopy (AFM) (1,2) is a useful new technique for observing DNA. The AFM can image conformations of DNA molecules (3–5), nucleosome conformations and substructure (6,7), unusual DNA structures such as G wires (8), the stoichiometry of a DNA–protein complex (9), the motion of DNA molecules as short as 300 base pairs (bp) in aqueous buffer (10,11) and DNA–enzyme interactions. AFM images of static DNA–enzyme interactions give information about enzyme locations on DNA and DNA bend angles (3,12), while dynamic images of DNA and active enzymes in aqueous buffer are initiating a new field of single molecule enzymology (10,11).

We present here new advances in AFM of DNA: the stable imaging of short single- and double-stranded DNA (dsDNA) molecules, images of triple-stranded DNA and single-stranded RNA homopolymers, images of 16 μm long lambda DNA molecules and images of DNA on silicon. The ability to image single-stranded DNA (ssDNA) molecules as short as 25 bp has already proved useful in our research on the covalent attachment of oligonucleotides to a surface.

MATERIALS AND METHODS

Substrates

Mica. Discs of mica (Ruby Mica; New York Mica Co., New York, NY) were glued to steel discs with 2-Ton® epoxy resin (Devcon Corporation; Wood Dale, IL) and cleaved with tape immediately before use.

Silicon. Oxidized silicon substrates were type P defect polished silicon wafers (orientation 1:1:0, 5–20 Ωcm) from the Semiconductor Processing Company (Boston, MA), broken into 0.5 inch squares. The silicon wafers were cleaned by immersion in 45% HNO_3 for 3 h, followed by a rinse consisting of sonicating three times in a large excess of MilliQ (Millipore Corp., Burlington, MA)-purified water for 5 min. The silicon wafers were blown dry with compressed air and glued with Spot-O-Glue (Avery, Azusa, CA) to steel disks. The silicon wafers should be used as soon as possible but can be stored in MilliQ-purified water for a few days. Freshly cleaned silicon is hydrophilic, but storing overnight in air can cause it to become hydrophobic and no longer bind DNA.

Nucleic acids

All dilutions and buffers were made with MilliQ-purified water. Nucleic acids were supplied by Pharmacia (Piscataway, NJ), except as noted otherwise.

Short ssDNAs. ssDNA 50 bases long was obtained from E.Delain (Institut G.Roussy, Villejuif, France). There were two different 50 base DNAs in this sample, with the following sequences: TCCTAGGGGCAAAAAAAAAATGTTCTGACTCCCCCCC-

* To whom correspondence should be addressed

CCCGCCGGTCACG and CGGCCAGTGCCAAGCTTGCATGCCTGCAGGTCGACTCTAGAGGATCCCCG (13). Intermolecular base pairing was minimized by diluting the 50 base DNA to 100 ng/µl in HEPES–Mg buffer (40 mM HEPES–KOH, 10 mM $MgCl_2$, pH 7.6) and heating for 5 min at 37°C.

DNA of 25 bases (Operon Technologies Inc., Alameda, CA) had the following sequence: GGCGCTGTGGCTGATTTCGATTTCGATAACC.

Short dsDNAs. dsDNAs of 200, 100 and 50 bp from BioVentures Inc. (Murfreesboro, TN) were supplied in water or in 10 mM Tris, 1 mM EDTA (10 ng/µl).

Short ssDNAs and dsDNAs were diluted in HEPES–Mg buffer unless noted otherwise. DNA of 200 bp was dialyzed against HEPES–Mg buffer using a 0.025 µm pore size filter (Millipore Corp., Bedford, MA).

Poly(A). The RNA homopolymer poly(A) was dissolved in water at a concentration of 30 ng/µl. The mean length of poly(A) molecules was ~400–600 bases, according to the supplier (Pharmacia).

DNA duplexes. The DNA duplexes poly(dA)·poly(dT) and poly(dG)·poly(dC) were diluted to 3 ng/µl in HEPES–Mg buffer. The mean lengths of poly(dA), poly(dT), poly(dC) and poly(dG) were ~150–350 bases, but the lengths of the resulting duplex DNAs were much longer, because the base pairing of molecules of heterogeneous lengths generates sticky ends that base pair to other molecules.

Lambda DNA. Lambda DNA was diluted to 1 ng/µl in HEPES–Mg buffer and heated for ~10 min at 65ºC.

ϕX-174 HincII digest DNA. ϕX-174 *Hinc*II digest DNA was diluted with water to 20 ng/µl. ϕX-174 *Hinc*II digest has dsDNA molecules with lengths of 79–1057 bp.

Plasmid DNA for oxidized silicon substrates. Double-stranded Bluescript II SK(+) plasmid DNA (2961 bp, 1 mg/ml in 10 mM Tris, 1 mM EDTA) from Stratagene (La Jolla, CA) was diluted with water to a concentration of 10 ng/µl.

Sample preparation

DNA on mica. For DNA in HEPES–Mg buffer 1 µl each DNA solution was incubated on a freshly cleaved mica substrate for 1–3 min, rinsed with water, dried with compressed air and further dried in a desiccator over P_2O_5. For DNAs in water 1 µl each DNA solution was pipetted onto freshly cleaved mica, dried with compressed air and further dried in a desiccator over P_2O_5.

Plasmid DNA on oxidized silicon. Bluescript plasmid DNA (10 µl) was placed on a silicon wafer for 15 s, blown dry with compressed air and further dried by placing in a desiccator and applying a vacuum of 150 mtorr for 2 min.

AFM imaging

AFM imaging was performed in tapping mode in an atmosphere of dry helium with a Nanoscope III (Digital Instruments, Santa Barbara, CA). Bungee cords were used for vibration isolation (11). The D scanner was used for all samples except lambda DNA, for which the J scanner was used. The D scanner was accurate to 8% in its *xy* calibration, based on measurements of images of a known grating. Standard 125 µm silicon cantilevers were obtained from Digital Instruments.

Images were processed by flattening to remove the background slope. The images in Figure 5D and E were also processed through a two-dimensional Fourier transform and large scale height corrugations in the image were removed. (Traces of these corrugations can be seen in Fig. 5D and in the lower left-hand corner of Fig. 5A, from which they were not removed.)

Heights of rod-shaped molecules and widths at half-height were measured using the Section/Cursor/Average commands in the Nanoscope software (version 3.12). Heights and widths at half-height were measured for globular molecules with the Section command.

Persistence lengths

To calculate apparent persistence lengths we followed a method developed for determining DNA persistence lengths from electron microscope (EM) images (14). Each DNA molecule was modeled as a chain of 10 nm segments (15). We graphed cosθ versus length (L), where θ is the angle between DNA segments separated by contour length L. The apparent persistence length a was calculated from the equation

$$\langle\cos\theta\ (L)\rangle = \exp(-L/2a)$$

where $\langle\cos\theta\ (L)\rangle$ is the arithmetic mean of cosθ for all DNA segments separated by contour length L.

Sequence analysis

Sequences of short ssDNAs were analyzed for possible intramolecular base pairing with the GCG Wisconsin Sequence Analysis Package (Genetics Computer Group, Madison, WI) using the Mfold and Foldrna programs (16).

RESULTS

Poly(A)

The RNA homopolymer poly(A) showed two conformations in AFM. Most of the RNA was present as short bent lumpy molecules (Fig. 1A). These molecules had lengths of the order of 100–300 nm and an apparent persistence length of the order of 40 nm.

Parts or all of a few molecules were much longer, straighter and less lumpy (arrow in Fig. 1B). These molecules had lengths of the order of 500–1500 nm and an apparent persistence length of the order of 600 nm. For comparison, the apparent persistence length of dsDNA was 80 nm (Fig. 1C).

The AFM images in Figure 1 are all for DNA or poly(A) in water dried onto mica. AFM images of poly(A) in 1 mM HEPES, pH 7, dried onto mica, showed lumpy molecules similar to those in Figure 1A, but no straight long molecules. Poly(A) in 1 mM HEPES could be dried without rinsing, as with poly(A) in water. In 10 mM HEPES buffer rinsing was necessary to remove the higher concentration of buffer salts; this rinsing removed the poly(A) as well.

Short dsDNAs and ssDNAs

Short dsDNA molecules of 100 and 200 bp were generally rod-like in shape (Fig. 2), while ssDNA molecules were globular (Fig. 3).

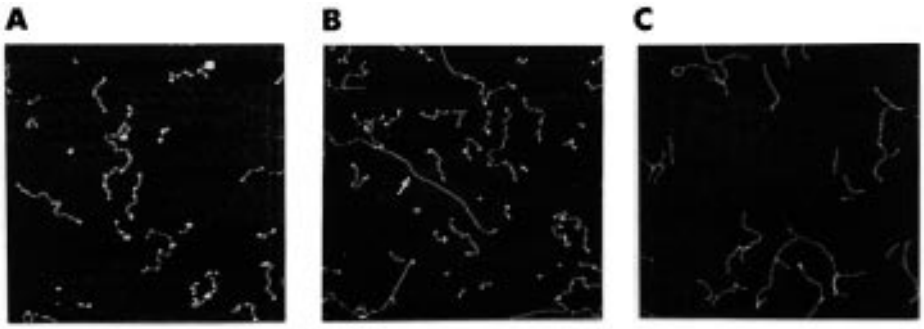

Figure 1. (**A**, **B**) Poly(A) in water dried onto mica shows primarily short bent lumpy molecules and a few long smooth straight molecules or segments of molecules (e.g. arrow in B). Mean length of poly(A) is 400–600 bases as supplied. (**C**) For comparison, dsDNA under the same conditions shows molecules intermediate in persistence length between the two molecular types of poly(A). The dsDNA is ϕX-174 *Hin*cII digest, whose molecular lengths are ~30–350 nm. All images are 1×1 μm.

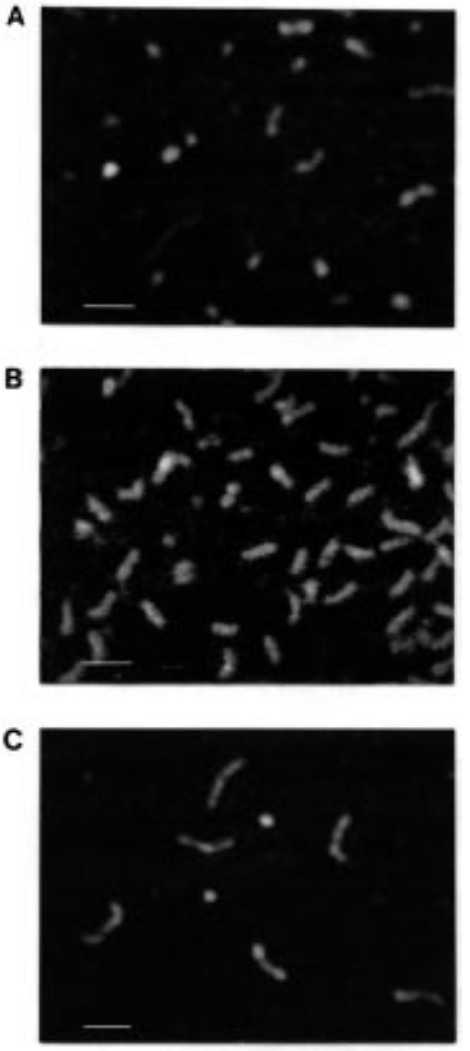

Figure 2. AFM images of short dsDNAs in air on mica. Bars are 50 nm. (**A**) 50 bp DNA, 10 ng/μl in 10 mM Tris, 1 mM EDTA, 170 mM $MgCl_2$. (**B**) 100 bp DNA, 2 ng/μl in 40 mM HEPES, 10 mM $MgCl_2$. (**C**) 200 bp DNA, 2 ng/μl in 40 mM HEPES, 10 mM $MgCl_2$.

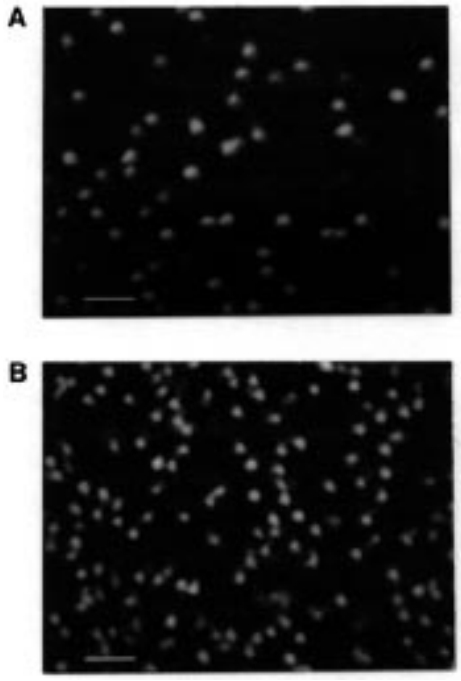

Figure 3. AFM images of short ssDNAs in air on mica. Bars are 50 nm. (**A**) 25 base DNA, 380 ng/μl in 40 mM HEPES, 10 mM $MgCl_2$. (**B**) 50 base DNA, 100 ng/μl in 40 mM HEPES, 10 mM $MgCl_2$.

dsDNA. Samples of 50 bp dsDNA did not show a consistent molecular conformation. Both globular and rod-like shapes were seen (Fig. 2A).

Samples of 100 bp dsDNA showed more homogeneous fields of rod-like molecules that were either straight or slightly bent (Fig. 2B). The measured lengths were 33 ± 5 nm.

Samples of 200 bp dsDNA showed curved rods with measured lengths of 59 ± 8 nm (Fig. 2C). Measured heights of 100 and 200 bp dsDNA were 0.4–0.6 nm. Measured widths were 11–12 nm.

ssDNA. Twenty-five and 50 base ssDNAs had globular conformations with mean measured diameters of 14 and 11 nm respectively (Fig. 3). The measured height of the molecules was ~1 nm. Images of 50 base ssDNA (Fig. 3B) show a more homogenous size distribution than those of the 25 base ssDNA

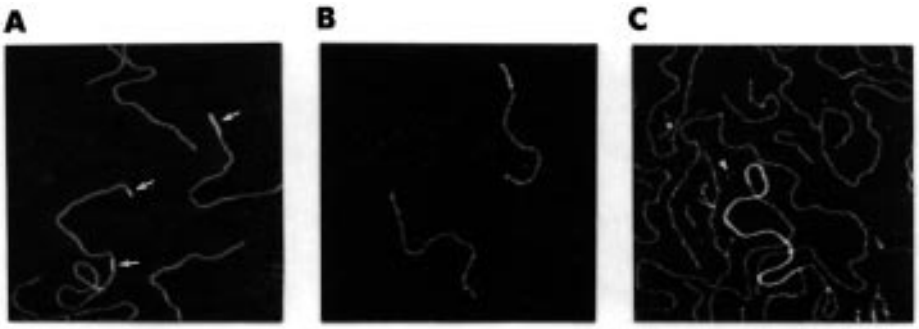

Figure 4. (**A**, **B**) Poly(dA)·poly(dT) and (**C**) poly(dG)·poly(dC) on mica, showing putative triple-stranded DNA segments and dsDNA. Arrows in (A) indicate DNA segments approximately twice as high as adjacent segments, in (B) the upper 50 nm of the upper molecule is a high segment, while in (C) the long curved segment is high. The high segments are probably triple-stranded DNA (ATT or GCC) formed when an overhanging pyrimidine strand folds back on the double helix. Arrowhead in (C) indicates a short bent lumpy segment that is probably ssDNA. Image sizes are 1 × 1 µm.

(Fig. 3A). It is possible that there was some aggregation of 25 base DNA molecules, leading to both its larger mean measured diameter and its less homogeneous distribution.

The Mfold program in the GCG software (16) gave possible secondary structures for intramolecular base pairing of the 25 and 50 base ssDNAs at 24°C, based on their base sequences. The first 12 bases of the 25 base DNA can form three base pairs with a six base loop. The 50 base DNA can form structures with one to three loops and 3–8 bp. These computer analyses are consistent with the globular shapes seen by AFM. These analyses do not prove that intramolecular loops were present, however, since they do not take into account the interaction with the mica surface or differences in ionic composition of the solution.

Short DNAs in propanol. Tapping AFM in propanol has not revealed any substructure in 100 and 200 bp DNA. This is not surprising, since AFM of dsDNA in propanol only rarely shows substructure as small as helix turns (11). AFM of short ssDNAs in propanol is even less informative, since background debris is more often present on samples in propanol and the background debris cannot be distinguished from the short ssDNA molecules.

Poly(dA)·poly(dT) and poly(dG)·poly(dC)

Images of these molecules showed primarily dsDNA, as expected (Fig. 4), with a few short branches that looked like ssDNA (e.g. arrowhead in Fig. 4C) or triple-stranded DNA (e.g. arrows in Fig. 4A). The molecules varied in length from tens of nanometers to a few microns. A number of the molecules were branched and some molecular aggregates had topologies that could not easily be followed.

The structures tentatively identified as triple-stranded DNA were twice as high as dsDNA (0.7 ± 0.2 nm for triple-stranded DNA versus 0.4 ± 0.1 nm for dsDNA), but similar in width (10 ± 1 nm). The measured heights varied among experiments, but the regions visually identified as triple-stranded DNA were 70–100% higher than the heights of the adjacent DNA.

Lambda DNA

Overlapping scans of lambda DNA give images of entire molecules with a good signal-to-noise ratio (Fig. 5). Figure 5B shows a rare circular lambda DNA molecule, while Figure 5A shows a linear molecule. Untangled linear molecules are difficult to find in most samples. Much more common are coiled or tangled molecules (Fig. 5C). Rarely, entire extended molecules can be imaged in a single 10 µm scan (Fig. 5D and E).

Plasmid DNA on silicon

Plasmid DNA in water is adsorbed onto oxidized silicon. Most of the plasmids were highly coiled, with only 5% being relaxed (Fig. 6). For comparison, the same sample preparation on mica gave 42% relaxed DNA. The plasmid density on silicon was 3.3 ± 1.5 plasmids/µm^2. The density of plasmids on silicon showed significant variation between samples and even within the same sample. There was little aggregation of DNA molecules.

Plasmid DNA (10 ng/µl) in HEPES–Mg buffer and in TE (10 mM Tris, 1 mM EDTA) could not be seen on silicon. Samples were rinsed with 2 ml MilliQ-purified water after DNA was put on the silicon, to prevent salt islands. This rinse apparently removed all DNA from the silicon.

The silicon surface was somewhat bumpy, with small 'pillars' of material rising >30 nm in height. Luckily, there were few pillars and the rest of the surface was smooth enough to visualize DNA. The number and density of pillars varied considerably between samples and even within the same sample. The root mean square (r.m.s.) roughness of the smooth areas is 0.15 ± 0.02 nm. Mica and silylated mica (AP-Mica) (17,18) are both smoother, with r.m.s. roughnesses of 0.06 ± 0.01 and 0.09 ± 0.01 nm respectively.

A number of unwashed silicon samples were also imaged. These untreated samples were highly variable and had more pillars than the HNO_3-washed silicon. Fewer plasmids were found on the untreated silicon (1.1 ± 2.2/µm^2), with most being coiled. This, coupled with the increase in pillar density and the variability of the untreated silicon makes the HNO_3 treatment worthwhile. Root mean square roughness of untreated silicon did not differ from that of acid-washed silicon.

Some silicon was cleaned with piranha solution (70% concentrated H_2SO_4, 30% concentrated H_2O_2). Silicon wafers were incubated in piranha solution at 90°C for 1 h, sonicated three times for 5 min in a large excess of MilliQ-purified water, then blown dry and glued to steel disks. Fewer pillars were seen, being replaced by smaller 'spikes' 30–70 nm in diameter and >5 nm in height. Like untreated silicon, few plasmids were found (0.8 ± 0.9/µm^2) and they were highly coiled. There were also surface

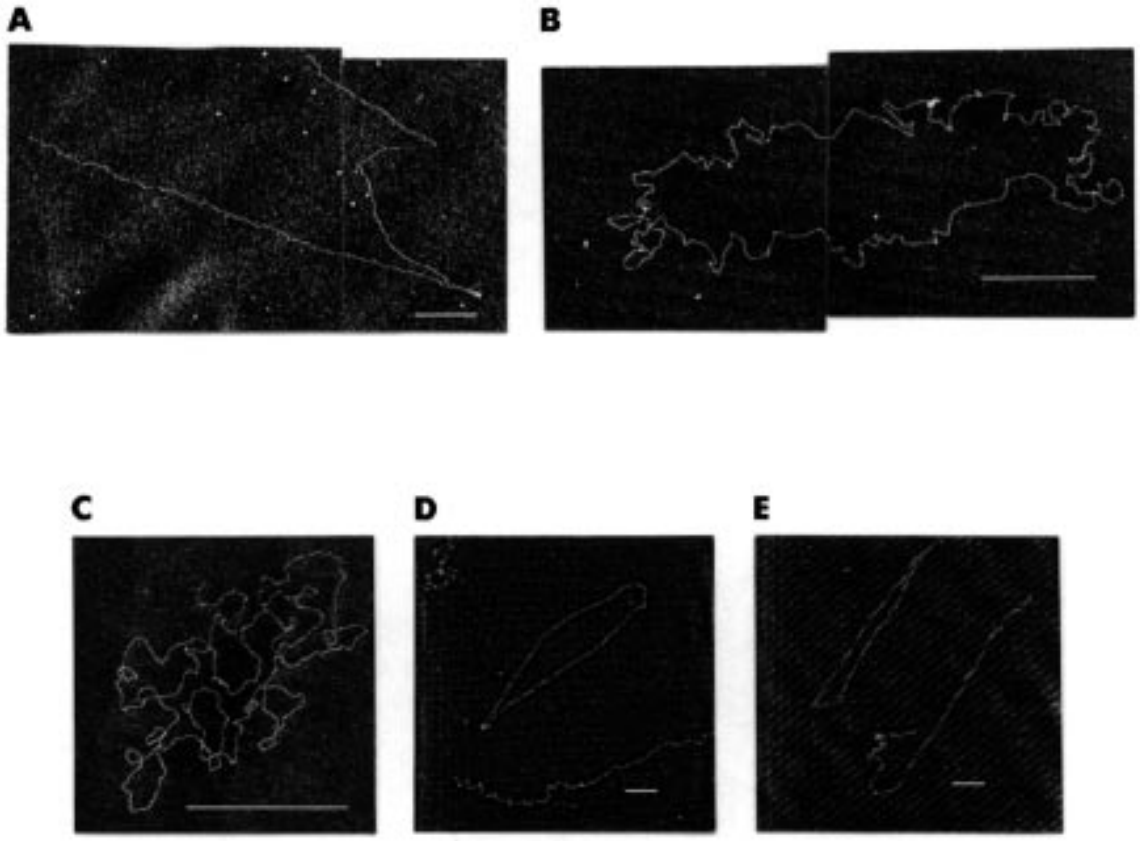

Figure 5. Entire lambda DNA molecules, 48 000 bp on mica. (**A**) Image of a well-extended linear molecule assembled from overlapping AFM images. (**B**) A rare circular molecule. Ethidium bromide (200 ng/µl) was present in the buffer. (**C**) Coiled or tangled molecules such as this one are most common. (**D**, **E**) Entire extended lambda DNA molecules captured in single 10 µm scans. Scale bars 1 µm.

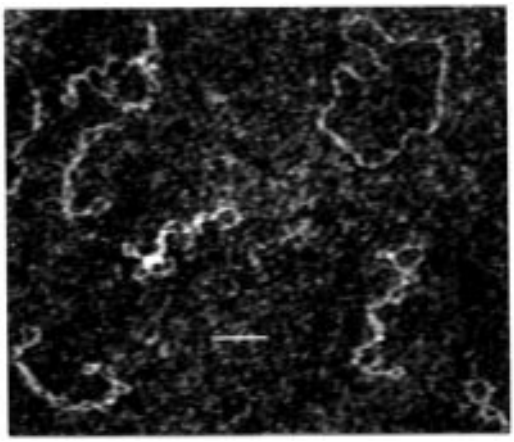

Figure 6. Bluescript plasmid DNA on silicon treated with HNO_3. Relaxed plasmids are quite uncommon, but one can be seen in the upper right-hand corner. Scale bar 100 nm.

features on the piranha-treated silicon that looked similar to the plasmids even in the absence of DNA.

DISCUSSION

Most AFM of nucleic acids has focused on dsDNA with lengths of several hundred to a few thousand base pairs bound to mica or modified mica. This work extends AFM of nucleic acids to DNA shorter than 100 bp and longer than 10 kbp, to ssRNA homopolymers, to triple-stranded DNA and to DNA on silicon. Images of DNA on silicon, although inferior to those on mica, are important for silicon-loving AFM users, who want to know whether silicon, which is a good substrate for Langmuir–Blodgett films (19,20), is also a good substrate for DNA.

Single- and double-stranded poly(A)

AFM imaging of well-extended ssDNA has been difficult. Even when denatured, single-stranded ϕX-174 DNA was extended to a length corresponding to only ~0.2 nm/base (21,22). If fully extended it should have had a base spacing at least as great as that of dsDNA, which is 0.3–0.34 nm/base pair. Single-stranded ϕX-174 DNA is capable of intramolecular base pairing, which may account for the difficulty of extending it fully.

In contrast, poly(A), being a homopolymer, cannot form intramolecular Watson–Crick base pairs. Thus poly(A) and other RNA and DNA homopolymers are good nucleic acids to use for AFM characterization of extended single-stranded nucleic acids. Single-stranded poly(A) can form a helix with two bases per turn (23). The AFM images of single-stranded poly(A) in Figure 1A show what looks like a jointed rod and may represent extended poly(A). The lengths of these molecules, ~100–300 nm, are consistent with an extended conformation, since molecular lengths are ~400–600 bases.

The apparent persistence length, 40 nm, is about half the value calculated for dsDNA deposited onto mica from solution in water. Persistence length is a measure of the flexibility of DNA. Persistence length is proportional to the rigidity of a polymer chain and is a measure of the distance that the polymer chain will continue in the same direction without bending (24,25). It is reasonable that a single-stranded polynucleotide, such as poly(A), would be more flexible than dsDNA. The absolute magnitude of the difference in flexibility is difficult to quantify, however, because any sequence-dependent curvature will give the appearance of a lower persistence length and the sequence of dsDNA is quite different from that of poly(A). The apparent persistence length of DNA is also dependent on the substrate to which the DNA is adsorbed (unpublished observations). This can be seen qualitatively by comparing Figure 1C and D in Bezanilla *et al.* (18).

The long, straight molecular segments in Figure 1B are probably double-stranded poly(A)$^+$, which forms at pH < 4, where the adenine N_1 is protonated (23). MilliQ-purified water is somewhat acidic, allowing some protonation of adenine N_1, although most of the poly(A) appears as the short bent molecules expected for single-stranded poly(A). Formation of double-stranded nucleic acids is a cooperative process, as would be expected from Figure 1B, since the double-stranded segments are never seen to be interrupted by single-stranded segments. The apparent persistence length of these molecules, ~600 nm, is much longer than that of dsDNA.

Since double-stranded poly(A)$^+$ has parallel strands (23), these double-stranded structures cannot form within single poly(A) molecules. This is again consistent with the hypothesis that the short bent lumpy molecules (Fig. 1A) are single-stranded polynucleotide.

Short dsDNA and ssDNA

Divalent cations have been used previously to immobilize long DNA molecules on mica (18,26–28). These cations form a bridge between the negatively charged phosphate backbone of DNA and the negatively charged surface of the mica. This technique has been used here to observe short synthetic molecules of dsDNA (50, 100 and 200 bp) and ssDNA (25 and 50 bases). The results show that molecules of ssDNA and dsDNA from 25 bases long can be observed with AFM in tapping mode in helium. Images were stable and molecules were not displaced by the tip.

dsDNA. dsDNA molecules form rods on mica. Measured lengths of 200 bp DNA are almost twice those of 100 bp DNA. These measured lengths are longer than the actual lengths of the molecules by an amount related to the size of the AFM tip. By subtracting the contribution of the tip size from the measured lengths we can estimate the base spacing in these DNA molecules and determine whether their conformations are A-DNA or B-DNA.

If the measured widths, 11–12 nm, are the sum of the actual width of dsDNA, 2–3 nm, plus the width of the tip, then the tip width is 9 nm and the corrected lengths of 200 and 100 bp DNA are 51 and 25 nm respectively. This corresponds to a spacing of 0.25 nm/bp, which is close to the values for A-DNA (0.26–0.29 nm/bp), but smaller than B-DNA (0.34 nm/bp) (23,29).

A-DNA is the dehydrated form, seen at relative humidities of 75% and lower, while B-DNA is the most common physiological form of DNA. Drying of the DNA samples in Figure 2 may have converted them to A-DNA. Prior results from our laboratory on AFM imaging of circular 3000 bp DNA showed that B-DNA lengths persisted even in propanol (30).

The discrepancy between previous results and those presented here may be due to the differences in DNA length. Long DNAs may bind to mica at many sites, which holds them as B-DNA even during drying, while short DNAs, which presumably bind to mica at fewer sites, shrink to A-DNA during sample dehydration. It would be interesting to test this hypothesis with a plot of DNA length versus DNA base spacing measured from AFM images, but there is at present little AFM data for DNA longer than 200 bp but shorter than 3000 bp.

Previously reported lengths from many laboratories for DNA in AFM correspond to base spacings of 0.28–0.34 nm/bp (22,26,27,30–37). These base spacings are all for DNAs longer than 200 bp, imaged under a variety of conditions. The smaller base spacing observed here for short DNAs is consistent with our model that short DNAs dried onto a substrate will shrink to a smaller base spacing than longer DNAs.

Measured heights were much smaller than 2.6 nm, which is the helix diameter of A-DNA. Heights of DNA in AFM are almost always <2 nm, except for contact AFM in aqueous solutions (2.5 nm; 30). Reported DNA heights vary from 0.5 to 1.9 nm in air and propanol (26,27,35,36,38). This discrepancy between the measured height and the expected value is probably due to compression of the DNA by the tip.

DNA of 50 bp did not give good AFM images of short rods. The molecules were not regular in shape; they appeared as rods of different sizes and as globular molecules. Three possible explanations may account for these results. First, these molecules are so short that, if their images have the same base spacing and tip broadening as seen for 100 and 200 bp DNA the measured dimensions would be only 12 × 22 nm, which may be too nearly globular to distinguish as a rod in AFM. Second, there may be some melting or separation of the DNA strands at the ends of the molecules, which would make their shape less rod-like. Third, there may be some end-to-end aggregation of DNA molecules. In Figure 2B, for example, the molecule in the upper right corner looks about twice as long as most of the other molecules. Such end-to-end aggregation could complicate interpretation of images, especially of molecules as short as 50 bp.

End-to-end aggregation is seen in AFM, especially with short DNA molecules, and is a consequence of the favorable free energies of base stacking in aqueous solution, which are comparable to *kT* (0.6 kcal/mol) (23). Other evidence for end-to-end aggregation of DNA is that even blunt-ended DNA molecules can be joined with ligase (39).

ssDNA. All the ssDNA molecules imaged had a globular shape. ssDNA molecules tend to fold back on themselves if nucleotides can base pair to form loops (40). The sequences of nucleotides in the 25 and 50 base DNAs allow base pairing and the formation of one or more loops. Moreover, Mg^{2+} neutralizes the electrostatic repulsion between negative charges in the phosphate backbone, so the presence of Mg^{2+} could facilitate folding of the molecules. ssDNA molecules had larger heights than dsDNA molecules, which also suggests that they may be forming loops.

There is evidence from scanning tunneling microscopy (STM) that short ssDNA molecules deposited electrochemically on gold do have a rod-like conformation (41). These DNAs were in an EDTA-containing buffer. The Mg^{2+} used in our AFM studies may

stabilize intramolecular base pairing by bridging phosphates in the backbone, giving the globular conformations seen by AFM. Mg^{2+} has been previously shown to induce intramolecular cross-bridges in dsDNA (42). It is also possible that electrochemical deposition may induce rod-like conformations of ssDNA, either by increasing repulsion between phosphates in the backbone or by stabilizing base stacking. The different surfaces, gold for STM and mica for AFM, may also affect the DNA conformations.

The globular molecules of 25 and 50 base ssDNA had approximately the same diameters. This can be explained from a calculation of the relative molecular diameters and from the contribution of the tip to measured widths. By assuming a sphere for these ssDNAs, if *R* is the radius of the 25 base DNA, then the radius of the 50 base DNA is 1.26*R*. Since the tip makes a large contribution to the measured widths, it is not possible to differentiate between molecules with such similar radii.

Double- and triple-stranded DNA: poly(dA)·poly(dT) and poly(dG)·poly(dC)

Images of the DNA duplexes poly(dA)·poly(dT) and poly(dG)·poly(dC) showed striking height elevations in some DNA segments that suggest triple-stranded DNA (Fig. 4). One would expect some triple-stranded DNA in these samples, since the annealing of purine and pyrimidine strands will sometimes result in single-stranded overhangs. Overhanging pyrimidine strands, poly(dT) and poly(dC), can fold back onto the dsDNA to form triple-stranded DNA in which the pyrimidine strands are antiparallel (23). In addition, poly(dG) strands can self-associate.

The measured heights of the elevated DNA segments were 70–100% higher than the adjacent DNA, which had heights typical for dsDNA in AFM. The widths were similar for putative dsDNA and triple-stranded DNA segments. Triple-stranded DNA may be less compressible than dsDNA. The shortest putative triple-stranded segment is 24 nm long (middle arrow in Fig. 4A), corresponding to ~70 bp.

Long DNA: lambda DNA

Lyubchenko's early images of lambda DNA showed the capability of AFM for imaging DNA molecules this long (~16 µm) (17). It is difficult to image long DNA molecules. As the scan size is increased to view such large molecules, the height fluctuations of the support increase and the width of the DNA in pixels decreases. Thus it is often difficult to trace the topography of the thread-like DNA molecules. The images in Figure 5 have a much better signal-to-noise ratio than earlier images.

The lambda DNA molecule in Figure 5B, assembled here from overlapping 5 µm scans, was also imaged in the Autoscan mode in a series of 3 µm images. Autoscan is an automated mode for capturing a number of images of fixed scan size and spacing and is a convenient way to collect images covering a large area. Autoscan will be increasingly useful now that AFM is being used in large scale screenings, such as the classification of chromosomes by volume measurement (43) and, potentially, chromosome mapping (44).

Plasmids on oxidized silicon

Uncoated DNA is too thin to resolve easily in AFM, except on the flattest substrates. Thus mica has generally been the substrate of choice (45), although glass coverslips were used for imaging nucleosomes, where the path of the DNA could be inferred in part from the path of the nucleosomes. The roughness of polished silicon, r.m.s. = 0.15 nm, is at the upper end of the tolerable range for imaging DNA. The advantage of silicon over mica is that silicon is conductive, while mica is an insulator. Thus silicon is a possible substrate for imaging DNA electrodeposited from solution, but silicon has limited usefulness for characterizing DNA samples in air, since DNA in buffer does not bind to silicon. Oxidized silicon has been a valuable substrate for imaging lipid films at molecular resolutions (19,20), because it does not have an ordered crystalline surface that can be confused with the ordered crystalline layers of lipids deposited onto it. Oriented lambda DNA has also been imaged on silylated silicon (46).

Plasmids were more coiled on silicon than on mica. Plasmids on AP-mica in some buffers are also more coiled than plasmids on mica (18). Since the topological properties of the DNA cannot change without breaking bonds, the observed differences in coiling must be due to differences in intramolecular interactions under different conditions.

CONCLUSION

Since AFM is proving to be a useful technique for imaging DNA, it is important to explore the limits of this technique. Two limits that are explored here are the types of DNA that can be reliably imaged and identified and the substrates that are flat enough for visualizing DNA by AFM. This work extends the range of DNAs imaged with AFM to: (i) short DNAs as small as 25 bases or 100 bp; (ii) long DNA from phage lambda, 48 000 bp, imaged here as clearly distinguished molecules; (iii) triple-stranded DNA, which measured twice as high as dsDNA; (iv) a well-extended single-stranded polynucleotide, poly(A). Additionally we have studied the use of oxidized silicon as a substrate.

ACKNOWLEDGEMENTS

We thank Robert Sinsheimer, Paul Hagerman, Stuart Lindsay, Paul Hansma, Monika Fritz and Jan Hoh for helpful discussions, T.C.Bruice and Ken Browne for helpful discussions and for providing some of the DNAs, Steve Wickert for assistance with the sequence analysis software and David Vie for expert technical assistance. This work was supported by NSF MCB 9317466 and Digital Instruments.

REFERENCES

1 Binnig,G., Quate,C.F. and Gerber,C. (1986) *Phys. Rev. Lett.*, **56**, 930–933.
2 Rugar,D. and Hansma,P.K. (1990) *Phys. Today*, **43** (10), 23–30.
3 Erie,D.A., Yang,G., Schultz,H.C. and Bustamante,C. (1994) *Science*, **266**, 1562–1566.
4 Samori,B., Siligardi,G., Quagliariello,C., Weisenhorn,A.L., Vesenka,J. and Bustamante,C.J. (1993) *Proc. Natl. Acad. Sci. USA*, **90**, 3598–3601.
5 Hansma,H.G., Browne,K.A., Bezanilla,M. and Bruice,T.C. (1994) *Biochemistry*, **33**, 8436–8441.
6 Yang,G., Leuba,S.H., Bustamante,C., Zlatanova,J. and Holde,K.v. (1994) *Struct. Biol.*, **1**, 761–763.
7 Martin,L.D., Vesenka,J.P., Henderson,E. and Dobbs,D.L. (1995) *Biochemistry*, **34**, 4610–4616.
8 Marsh,T.C., Vesenka,J. and Henderson,E. (1995) *Nucleic Acids Res.*, **23**, 696–700.
9 Wyman,C., Grotkopp,E., Bustamante,C. and Nelson,H.C.M. (1995) *EMBO J.*, **14**, 117–123.
10 Bezanilla,M., Drake,B., Nudler,E., Kashlev,M., Hansma,P.K. and Hansma,H.G. (1994) *Biophys. J.*, **67**, 2454–2459.

11 Hansma,H.G., Bezanilla,M., Laney,D.L., Sinsheimer,R.L. and Hansma,P.K. (1995) *Biophys. J.*, **68**, 1672–1677.
12 Rees,W.A., Keller,R.W., Vesenka,J.P., Yang,C. and Bustamante,C. (1993) *Science*, **260**, 1646–1649.
13 Delain,E. (1995) *STM–AFM and Biological Objects*. Fondation Fourmentin-Guilbert, Noisy le Grand, pp. 4.21–4.23.
14 Frontali,C., Dore,E., Ferrauto,A., Gratton,E., Bettini,A., Pozzan,M.R. and Valdevit,E. (1979) *Biopolymers*, **18**, 1353–1373.
15 Hansma,H.G., Laney,D.E., Revenko,I., Kim,K. and Cleveland,J.P. (1995) In Sarma,R.H. and Sarma,M.H. (eds), *Ninth Conversation in Biomolecular Stereodynamics*. Adenine Press, Albany, NY, in press.
16 Zuker,M. and Steigler,P. (1981) *Nucleic Acids Res.*, **9**, 133–148.
17 Lyubchenko,Y.L., Shlyakhtenko,L.S., Harrington,R.E., Oden,P.I. and Lindsay,S.M. (1993) *Proc. Natl. Acad. Sci. USA*, **90**, 2137–2140.
18 Bezanilla,M., Manne,S., Laney,D.E., Lyubchenko,Y.L. and Hansma,H.G. (1995) *Langmuir*, **11**, 655–659.
19 Radmacher,M., Tillmann,R.W., Fritz,M. and Gaub,H.E. (1992) *Science*, **257**, 1900–1905.
20 Schwartz,D.K., Garnaes,J., Viswanathan,R. and Zasadinski,J.A.N. (1992) *Science*, **257**, 508–511.
21 Hansma,H.G., Sinsheimer,R.L., Li,M.Q. and Hansma,P.K. (1992) *Nucleic Acids Res.*, **20**, 3585–3590.
22 Thundat,T., Allison,D.P., Warmack,R.J., Doktycz,M.J., Jacobson,K.B. and Brown,G.M. (1993) *J. Vacuum Sci. Technol. A*, **11**, 824–828.
23 Saenger,W. (1984) *Principles of Nucleic Acid Structure*. Springer-Verlag, New York, NY.
24 Hagerman,P.J. (1988) *Annu. Rev. Biophys. Chem.*, **17**, 265–286.
25 Crothers,D.M. (1992) In Kyogoku,Y. and Nishimura,Y. (eds), *Molecular Structure and Life*. Japan Scientific Society Press, Tokyo, Japan and CRC Press, Boca Raton, FL, pp. 67–77.
26 Vesenka,J., Guthold,M., Tang, C.L., Keller,D., Delaine,E. and Bustamante,C. (1992) *Ultramicroscopy*, **42–44**, 1243–1249.
27 Bustamante,C., Vesenka,J., Tang,C.L., Rees,W., Guthold,M. and Keller,R. (1992) *Biochemistry*, **31**, 22–26.
28 Thundat,T., Allison,D.P., Warmack,R.J., Brown,G.M., Jacobson,K.B., Schrick,J.J. and Ferrell,T.L. (1992) *Scanning Microsc.*, **6**, 911–918.
29 Dickerson,R.E. (1983) *Sci. Am.*, **249** (6), 94–111.
30 Hansma,H.G., Bezanilla,M., Zenhausern,F., Adrian,M. and Sinsheimer,R.L. (1993) *Nucleic Acids Res.*, **21**, 505–512.
31 Murray,M.N., Hansma,H.G., Bezanilla,M., Sano,T., Ogletree,D.F., Kolbe,W., Smith,C.L., Cantor,C.R., Spengler,S., Hansma,P.K. and Salmeron,M. (1993) *Proc. Natl. Acad. Sci. USA*, **90**, 3811–3814.
32 Shaiu,W.-L., Larson,D.D., Vesenka,J. and Henderson,E. (1993) *Nucleic Acids Res.*, **21**, 99–103.
33 Yang,J., Takeyasu,K. and Shao,Z. (1992) *FEBS Lett.*, **301**, 173–176.
34 Zenhausern,F., Adrian,M., tenHeggler-Bordier,B., Emch,R., Jobin,M., Taborelli,M. and Descours,P. (1992) *J. Struct. Biol.*, **108**, 69–73.
35 Schaper,A., Pietrasanta,L.I. and Jovin,T.M. (1993) *Nucleic Acids Res.*, **21**, 6004–6009.
36 Thundat,T., Allison,D.P. and Warmack,R.J. (1994) *Nucleic Acids Res.*, **22**, 4224–4228.
37 Muzzalupo,I., Nigro,C., Zuccheri,G., Samori,B., Quagliariello,C. and Buttinelli,M. (1995) *J. Vacuum Sci. Technol. A*, **13**, 1752–1754.
38 Delain,E., Fourcade,A., Poulin,J.-C., Barbin,A., Coulaud,D., Cam,E.L. and Paris,E. (1992) *Microsc. Microanal. Microstruct.*, **3**, 457–470.
39 Sgaramella,V. and Khorana,H.G. (1972) *J. Mol. Biol.*, **72**, 427.
40 Watson,J.D., Hopkins,N.H., Roberts,J.W., Steitz,J.A. and Weiner,A.M. (1987) In Gillen,J.R. (ed.), *Molecular Biology of the Gene*, 4th Edn. Benjamin/Cummings Publishing, Menlo Park, CA, Vol. I, pp. 240–281.
41 Jing,T.W., Jeffrey,A.M., DeRose,J.A., Lyubchenko,Y.L., Shlyakhtenko,L.S., Harrington,R.E., Appella,E., Larsen,J., Vaught,A., Rekesh,D., Lu,F.-X. and Lindsay,S.M. (1993) *Proc. Natl. Acad. Sci. USA*, **90**, 8934–8938.
42 Bednar,J., Furrer,P., Stasiak,A., Dubochet,J., Engelman,E.H. and Bates,A.D. (1994) *J. Mol. Biol.*, **235**, 825–847.
43 McMaster,T.J., Baker,A.A., Winfield,M.O. and Miles,M.J. (1995) *Eighth International Conference on Scanning Tunneling Microscopy/Spectroscopy and Related Techniques*. American Vacuum Society, Snowmass Village, CO, p. 191.
44 Allison,D.P., Doktycz,M.J., Kerper,P.S., Thundat,T. and Warmack,R.J. (1995) *Eighth International Conference on Scanning Tunneling Microscopy/Spectroscopy and Related Techniques*. American Vacuum Society, Snowmass Village, CO, p. 152.
45 Hansma,H.G. and Hoh,J. (1994) *Annu. Rev. Biophy. Biomol. Struct.*, **23**, 115–139.
46 Bensimon,A., Simon,A., Chiffaudel,A., Croquette,V., Heslot,F. and Bensimon,D. (1994) *Science*, **265**, 2096–2098.